

On the Achievable Throughput of Energy-Harvesting Nanonetworks in the Terahertz Band

Xin-Wei Yao , Member, IEEE, Chao-Chao Wang, Wan-Liang Wang, and Josep Miquel Jornet, Member, IEEE

Abstract—In this paper, the maximum achievable throughput of electromagnetic nanonetworks in the terahertz (THz) band (0.1–10 THz) is comprehensively investigated. On the one hand, the peculiarities of the THz-band channel are taken into account by capturing the impact of the molecular absorption loss on the signal propagation. On the other hand, a two-state medium access control protocol is utilized to reflect the behavior of energy-harvesting nano-devices with constrained harvesting rate and maximum transmission power P_0 . An ad-hoc nanonetwork is considered with n identical randomly located nano-devices, and each is capable of utilizing W Hz of bandwidth. When the node density of nanonetworks is low, the achievable throughput is $O(W P_0 ((n \log n)^{\alpha_{spr}-1/2} / \exp((\alpha_{abs}/(n \log n)^{1/2}))))^{1/2}$, where α_{spr} and α_{abs} refer to the spreading loss coefficient and the molecular absorption loss coefficient. When the node density of nanonetworks is very high, the interference among nano-devices governs the network behavior and the achievable throughput becomes $O((W^2 P_0 / I(n)) ((n \log n)^{\alpha_{spr}-1/2} / \exp((\alpha_{abs}/(n \log n)^{1/2}))))^{1/2}$. For both the cases, the upper boundaries of the achievable throughput are analytically derived, and the numerical results are provided. Numerical results illustrate that the molecular absorption loss plays the main role when the nanonetwork is sparse, and the interference dominates when the nanonetwork node density is very high.

Index Terms—Throughput, network capacity, terahertz communications, nanonetworks.

I. INTRODUCTION

NANOTECHNOLOGY is providing the engineering community with the required tools to develop miniaturized devices, i.e., nano-devices, which are able to perform specific tasks at the nanoscale, such as sensing and actuation. Due to their very limited individual capabilities, large assemblies of nano-devices are envisioned to perform more complex tasks in a distributed manner [1], [2]. Recent developments in graphene-based nano-electronics, nano-photonics and nano-plasmonics [3] enable electromagnetic (EM) communication among nano-devices in the Terahertz (THz) band (0.1–10 THz) [4], [5]. This very high

frequency band is becoming very attractive to the wireless research community, not just for nanonetworks, but also as a candidate technology for 5G cellular systems [6]. The THz-band can provide users with unprecedentedly large bandwidths, ranging from tens of GHz to a few THz [7]. However, this bandwidth comes at the cost of a high path loss. Given the limited transmission power of THz sources, the communication distance might be compromised for long range THz communications, unless highly directional antennas are used in transmission and reception. In any case, this is not a problem for nanonetworks, which benefit from the compact size of THz transceivers and antennas and do not require long range communications.

There are many peculiarities in EM nanonetworks which introduce new challenges and many opportunities across the protocol stack. In [8], the main phenomena affecting the propagation of EM signals in the THz band was modeled and analyzed. Particularly, molecular absorption loss plays a key role in the propagation of THz signals, in addition to the conventional spreading loss, which is also in lower frequency wireless communication systems. For distances much below one meter, which is the expected single-hop communication distance of individual nano-device, the THz band behaves as a single transmission window almost 10 THz wide [8], [9]. As shown in [10], this very large bandwidth enables novel femtosecond-long pulse-based communication schemes suitable for the limited resources of nano-devices, able to support multi Gigabits-per-second (Gbps) and up to a few Terabits-per-second (Tbps) links. However, the very small energy capacity of nano-batteries and the need for energy-harvesting systems [11] pose a major bottleneck in the performance of nanonetworks [12]. Ultimately, there are many interdependencies between the nano-device capabilities, the THz channel behavior and the physical and link layers solutions, which shape the achievable throughput or capacity of nanonetworks [13].

As a critical parameter, the network capacity or achievable throughput needs to be investigated in-depth for the design and evaluation of nanonetworks in the THz band. To date, the study of the capacity of wireless networks has been conducted for different types of networks under different system assumptions [14]. On the one hand, for traditional RF wireless networks, under the assumption of infinite bandwidth W , the network capacity has been analyzed for systems under the noninterference model [15], with power constrained devices [16], [17], directional antennas [18], [19], or multirate networks [20]. On the other hand, for millimeter wave wireless

Manuscript received August 4, 2017; accepted November 15, 2017. Date of publication November 22, 2017; date of current version December 21, 2017. This work was supported by the National Natural Science Foundation of China under Grant 61379123, Grant 61402414, and Grant 61772471. The associate editor coordinating the review of this paper and approving it for publication was Prof. Dongsoo Har. (Corresponding author: Xin-Wei Yao.)

X.-W. Yao, C.-C. Wang, and W.-L. Wang are with the College of Computer Science and Technology, Zhejiang University of Technology, Hangzhou 310023, China (e-mail: xwyao@zjut.edu.cn; ccwang@zjut.edu.cn; ww@zjut.edu.cn).

J. M. Jornet is with the Department of Electrical Engineering, University at Buffalo, The State University of New York, Buffalo, NY 14260 USA (e-mail: jmjornet@buffalo.edu).

Digital Object Identifier 10.1109/JSEN.2017.2776301

1558-1748 © 2017 IEEE. Personal use is permitted, but republication/redistribution requires IEEE permission.
See http://www.ieee.org/publications_standards/publications/rights/index.html for more information.

networks, molecular absorption loss and directional transmission are taken into consideration [21], [22]. However, as a result of the main peculiarities of THz nanonetworks, such as the molecular absorption loss, constrained transmission power and limited energy harvesting rate, none of the existing works can be directly mapped to the nanonetworking paradigm.

In this paper, we develop a general mathematical framework and analytically investigate the maximum achievable throughput of EM nanonetworks in the THz band. The peculiarities of the THz band in signal propagation, especially the molecular absorption loss, as well as the limitations of energy harvesting systems when using piezoelectric nano-generators are comprehensively captured in our analysis. As a result, we provide a closed-form expression for the behavior of the achievable throughput as a function of the spreading loss coefficient α_{spr} , the molecular absorption loss coefficient α_{abs} , the energy-harvesting-limited maximum transmission power P_0 and the available bandwidth W . More specifically, our mathematical framework accounts for the following peculiarities.

First, in order to capture the impact of the molecular absorption, we incorporate an exponential term to the common path loss function. This exponential term includes the molecular absorption loss coefficient α_{abs} , which depends on the transmission frequency and the molecular composition of the medium. At THz frequencies, this coefficient is dominated by water vapor molecules, as opposed to that in millimeter wave wireless systems, which is mainly affected by oxygen.

Second, in order to capture the impact of maximum transmission power P_0 and energy harvesting rate λ_{harv} in nano-devices, we consider a two-state medium access control (MAC) protocol, namely, state can be in energy harvesting and data transmission/reception (HTR) simultaneously or only energy harvesting (HS). On the one hand, the energy harvesting rate and consumption rate jointly determine the allocation of time in each state, which will affect the available energy. On the other hand, the maximum transmission power constrained by the harvested energy will finally limit the achievable throughput of THz nanonetworks.

Third, by introducing two metrics, energy efficiency and spectrum efficiency, we establish the relation between the above peculiarities and the achievable throughput, and present the upper bound of the achievable throughput of nanonetworks in the THz band. In detail, when the nanonetwork node density is low, the achievable throughput is

$$O \left(W P_0 \frac{(n \log n)^{\frac{\alpha_{spr}-1}{2}}}{\exp \left(\frac{\alpha_{abs}}{\sqrt{n \log n}} \right)} \right)^{\frac{1}{2}},$$

whereas when the nanonetwork node density is very high, the interference $I(n)$ among nano-devices should be considered, and then the achievable throughput is

$$O \left(\frac{W^2 P_0 (n \log n)^{\frac{\alpha_{spr}-1}{2}}}{I(n) \exp \left(\frac{\alpha_{abs}}{\sqrt{n \log n}} \right)} \right)^{\frac{1}{2}}.$$

These bounds demonstrate that the achievable throughput increases with node density n , available channel bandwidth W

and maximum transmission power P_0 , but decreases with the molecular absorption loss coefficient α_{abs} . These results are evaluated, and also compared with the existing results without considering the molecular absorption loss.

The remainder of this paper is organized as follows. In Sec. II, we discuss the related works. The system model, including path loss, energy harvesting and MAC protocol for nanonetworks, is presented in Sec. III. In Sec. IV, we derive an upper bound of the achievable throughput imposed by absorption and noise, in the case of low node density. In Sec. V, we derive the upper bound of the achievable throughput by focusing on the interference among nano-devices when the node density is very high. The proposed models are numerically evaluated through the comparison with the existing works in Sec. VI. Finally, the paper is concluded in Sec. VII.

II. RELATED WORKS

The objective of this paper is to comprehensively analyze the effect of the features of nano-devices capabilities, THz channel properties, and physical and link layers solutions on the achievable throughput of nanonetworks in the THz band. This requires contrasting the assumptions and results of the existing works with our results. Without loss of generality, the main relevant works are discussed next.

In the seminal work in [15], the throughput of wireless networks is analyzed under a noninterference protocol, i.e., assuming that nodes have full control on their transmission power so to avoid interference between them, and without considering the energy limitation in ad-hoc networks. As a result, the network capacity, which is bounded by $O(W/\sqrt{n \log n})$, decreases as a function of the node density n , but increase with the available channel bandwidth W . Based on the above analysis, in [16], more related physical layer properties, such as the limited transmission power and the use of rate adaptation, are taken into account to alleviate the interference in an ultra-wide band ad-hoc wireless network. Consequently, the network capacity increases with the node density n and the maximum transmission power P_0 , i.e., $O(P_0(\sqrt{n \log n})^{\alpha-1})$, where $\alpha = \alpha_{spr}$ refers to spreading loss coefficient. The above same problem is revisited in [17], and finally, a stronger result through different mathematical derivations for the power constrained network capacity is given by $O(P_0(\sqrt{n \log n})^{\alpha-1})$.

However, the above results are obtained under the assumption of infinite bandwidth. Actually, even in THz networks with the whole THz band as a transmission window, the available bandwidth W cannot be considered to go to infinity, because nanonetworks will expectedly have very large node densities, resulting in limited available bandwidth per node. In addition to all these, the molecular absorption loss in high frequency networks (such as THz networks and millimeter wave networks) makes the derivation of network capacity more complicated [14], [22]. Moreover, the energy limitations in nano-devices, both limited energy capacity and low energy harvesting rate, significantly affect the available throughput. This extremely increases the difficulties to explore the final network capacity expression with the physical layer peculiarities of THz signal. Next, we jointly capture all these peculiarities

on the analysis of the achievable throughput of nanonetworks in the THz band.

III. SYSTEM MODEL

The objective of this section is to demonstrate the peculiarities of THz nanonetworks from the aspects of physical layer, link layer as well as nano-devices capabilities. Particularly, in the physical layer, the path loss of THz signal is briefly summarized. For the energy limitations in nano-devices, an energy harvesting system with piezoelectric nano-generator is considered. In the link layer, a two-state MAC protocol is considered to guarantee the perpetual operation of the nanonetwork. These three features mainly and jointly dominate the achievable throughput of nanonetworks in the THz band.

A. Path Loss

The path loss measures the power reduction of an EM wave as it propagates through the medium. In EM nanonetworks, the total path loss for a traveling EM wave in the THz band is contributed by the spreading loss (similar in the low frequency wireless networks) and the molecular absorption loss. The spreading loss is introduced by the expansion of the wave over transmission distance, while the absorption loss is caused by the absorption of molecules in the transmission medium. A modified Friis equation to calculate the path loss of THz band is written as follows [8], [13]:

$$H_{loss} = \left(\frac{4\pi df}{c}\right)^{\alpha_{spr}} \exp(\alpha_{abs}d) = \frac{d^{\alpha_{spr}}}{C_0} \exp(\alpha_{abs}d), \quad (1)$$

where f is the transmission frequency, d is the distance between the transmitter and receiver, c is the speed of light in the vacuum, and the constant $C_0 = \left(\frac{c}{4\pi f}\right)^{-\alpha_{spr}}$. α_{spr} refers to the spreading loss coefficient, which equals to 2 for spherical omni-directional transmission in free space. α_{abs} refers to the molecular absorption loss coefficient. The detailed calculation of α_{abs} can be found in [8] and [13]. Briefly, this coefficient depends on the transmission frequency and the molecular composition of the medium. By utilizing the radiation transfer theory and the information of the HITRAN database, α_{abs} can be correspondingly obtained for different network scenarios with different channel molecular compositions. At THz frequencies, the absorption loss coefficient is mainly determined by the percentage of water vapor molecules or simply the humidity of the medium. (Note that multi-path fading is not included in this section because there are no conclusive multi-path channel models for THz networks [9], and, in any case, the impact of multi-path depends on the specific modulation being used. For example, if 100-femtosecond-long pulses are transmitted, different propagation paths are distinguishable provided that they are originated 30 micrometers apart. Therefore, we acknowledge that capturing multi-path and fading is relevant, but will not fundamentally change the results in this work.)

In addition to the loss, molecular absorption also results in noise. This noise is frequency dependent, correlated with the transmitted signal and can be modeled with a Gaussian process. However, there are other noise sources, mainly, the electronic noise at the receiver, which might dominate the

total noise. However, as of today, the noise models in nano-electronic, nanophotonic or nanoplasmonic devices are not conclusive nor readily available. Because of this, in this paper, we model the noise as a Gaussian process with mean zero, and variance N_0 .

B. Energy Harvesting With A Piezoelectric Nano-Generator

Besides the molecular absorption loss, the constrained energy in nano-devices is another major challenge that extremely limits the performance of THz nanonetworks. In particular, the very small capacity of nano-batteries requires nano-nodes to harvest energy from the surrounding environment to guarantee their proper operation. Within the last decade, energy harvesting nano-systems have been successfully designed to realize the energy conversion at nanoscale, such as piezoelectric nano-generators [11], ultrasound technology [23] and chemical reactions [24].

In this paper, we consider a piezoelectric nano-generator to harvest and convert mechanical energy into electrical energy. The harvested energy is stored in a nano-capacitor (or an array of nano-capacitors) to power the circuits of the nano-devices. The maximum energy that can be stored is given by

$$E_{max}^{harv} = \max \left\{ \frac{1}{2} C_{cap} (V_{cap}(n_{cyc}))^2 \right\} = \frac{1}{2} C_{cap} V_g^2, \quad (2)$$

where C_{cap} and V_{cap} refer to the total capacitance and the voltage of the capacitor, respectively. V_g is the voltage at which the capacitor is charged. n_{cyc} refers to the number of charging cycles. The voltage V_{cap} of the charging capacitor can be computed as a function of the number of cycles n_{cyc} is given by [12]

$$V_{cap}(n_{cyc}) = V_g \left(1 - e^{-\frac{n_{cyc} \Delta Q}{V_g C_{cap}}} \right). \quad (3)$$

Therefore, the maximum energy can be obtained after a number of cycles $n_{cyc}(E_{max}^{harv})$. With these premises, the energy harvesting rate λ_{harv} in Joule per second can be computed as follows [12], [13]:

$$\lambda_{harv} = \frac{1}{t_{cyc}} \cdot \frac{\partial E_{cap}}{\partial n_{cyc}} = \frac{V_g \Delta Q}{t_{cyc}} \left(e^{-\frac{\Delta Q n_{cyc}}{V_g C_{cap}}} - e^{-2\frac{\Delta Q n_{cyc}}{V_g C_{cap}}} \right), \quad (4)$$

where $\frac{\partial E_{cap}}{\partial n_{cyc}}$ is the energy increase of the capacitors in each cycle and t_{cyc} is one charging cycle length. ΔQ is the amount of electric charge obtained from a single cycle. However, note that there is no need to wait for the nano-capacitor to be fully recharged to consume its energy. In particular, V_g , ΔQ , and C_{cap} are technology parameters. While there are several existing works focused on energy modeling [11], [12], we keep our analysis general to remain valid even as technology advances.

C. Two-State MAC Protocol

Even with energy harvesting, the energy problem in nano-devices still exists. On the one hand, the real-time harvested energy may not be enough to support continuous data transmission, and a Harvest-Store-Use (HSU) operation architecture is preferred to a Harvest-Use (HU) architecture. In detail,

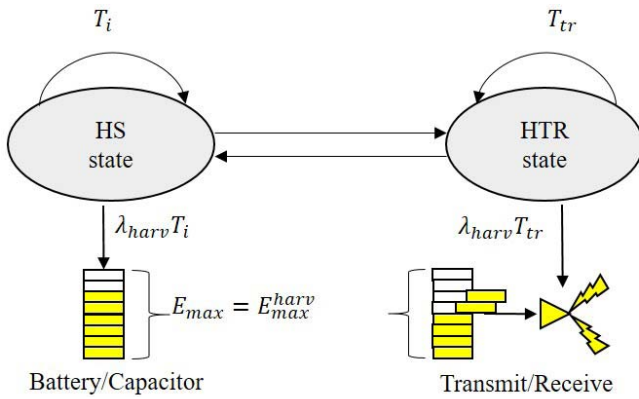


Fig. 1. Two-states MAC mechanism.

HSU refers to the architecture that the harvested energy is firstly stored into the battery before being used, while HU refers to the architecture that the harvested energy is high enough to be used directly to power the nano-device in real-time. On the other hand, for each nano-device, it is not necessary to be always in the active state, i.e., in the state of transmitting or receiving. Therefore, compared with the existing physical layer aware MAC protocol [25] or Receiver-Initiated MAC protocol [26], state controlled MAC protocols are more general to investigate the energy limitation for analyzing the achievable throughput of nanonetworks.

In this paper, we propose a simple and general MAC protocol with two states as shown in Fig. 1. From the perspective of networks, there are only two states for each node, i.e., busy and idle. Therefore, with the peculiarities of nanonetworks, the proposed MAC protocol is designed with two states as follows. The left state is Harvest-Store (HS) state, which refers to the nano-device in the state of only harvesting energy, no data transmission or reception, all the harvested energy is stored into the batteries. The right state is Harvest-Transmit/Receive (HTR) state, which refers to the nano-device in the state of harvesting and transmitting or receiving data simultaneously. As in HTR state, the harvested energy will be utilized by the transceiver directly. In addition, when the harvested energy is not sufficient, some energy from the battery would be required to support the data communication.

In detail, when there is no data to be transmitted or received, a nano-device transfers to the HS state for saving energy while harvesting energy. The nano-device switches to the HTR state when it needs to transmit or receive data and has sufficient energy. The time period in each state is dynamically adapted according to the network traffic. More specifically, T_i is the time period a node stays in HS state. T_i needs to be adapted according to the network traffic conditions. Without loss of generality, this adaption is estimated as a similar way to that of the TCP congestion window update algorithm [27]. Thus, after the data communication in HTR state, the value of time period $\{T_i, i \geq 1\}$ is initially set to one second when $i = 0$, i.e., $T_0 = 1$, and increases as follows:

$$T_i = \begin{cases} 2T_{i-1} & 2T_{i-1} \leq W_{ts} \\ \min\{T_{i-1} + 1, T_{\max}\} & 2T_{i-1} > W_{ts}, \end{cases} \quad (5)$$

where T_{\max} refers to the maximum time period that a node stays in HS state. W_{ts} refers to a threshold which decides the double increase period and linear increase period. Note that when the data transmission or reception is finished, i.e., the HTR state is done, the node will switch to the HS state and reset $T_i = 1$. W_{ts} is adaptive to the time between transmissions, and can be obtained as

$$W_{ts_new} = (1 - a)W_{ts_old} + a \cdot \frac{\sum T_i}{T_{tr}}, \quad (6)$$

where $0 < a < 1$, and $\sum T_i$ is the sum of the previous time intervals in the HS state, T_{tr} is the required time period to transmit data in HTR state. So $\frac{\sum T_i}{T_{tr}}$ refers to the estimated traffic condition, which depends on the network traffic. For example, under the heavy traffic condition, the time period in HS state needs to be reduced to guarantee the data transmission. Therefore, the new threshold W_{ts_new} decreases as a result of a large value of T_{tr} (The calculation of T_{tr} will be presented in Sec. IV). Moreover, due to the limitation of the processing capabilities of nano-devices, only uncomplicated MAC protocols are recommended. Other enhancements and more complex MAC protocols can be found in [27] and [28], but these are beyond the scope of this paper.

D. SINR Model

The performance of the nanonetwork ultimately depends on the received signal power at each node and how it compares to the noise and multi-user interference. Let $\{X_k\}$ be the subset of nodes simultaneously transmitting at some time instant over a certain sub-channel, where k refers to the node index. Let $P_{ij} \geq 0$ be the transmission power chosen by node X_i over the link from node X_i to node X_j , i.e., link $X_i \rightarrow X_j$. g_{ij} refers to the attenuation as a result of path loss over the link, given by (1), especially the molecular absorption loss in the THz band, and it can be simplified as a function of transmission distance by [16], [17]

$$g_{ij} = F(|X_i - X_j|) \simeq \frac{1}{|X_i - X_j|^{\alpha_{spr}}} \exp(-\alpha_{abs} |X_i - X_j|) \quad (7)$$

where $|X_i - X_j|$ refers to the transmission distance between node X_i and node X_j , α_{spr} refers to the spreading loss coefficient, α_{abs} refers to the molecular absorption coefficient, as described in Sec. III-A. The data transmitted from source node X_i is successfully received by the corresponding destination node X_j if and only if the minimum Signal-to-Interference-and-Noise Ratio (SINR) is satisfied [17], which is given by

$$\frac{P_{ij} g_{ij}}{WN_0 + \sum_{k \in \mathfrak{N}, k \neq i} P_{kj} g_{kj}} \geq SINR_{\min}, \quad (8)$$

where P_{ij} is the transmission power from node i to node j , $SINR_{\min}$ is the required minimum SINR, W is the channel bandwidth. At this point, we propose to distinguish two different working scenarios. On the one hand, when the node density is low, or, when the multi-user interference can be effectively neglected either because of the very high path-loss between nodes or because of the very large available

bandwidth at THz Band, (8) can be rewritten as:

$$\frac{P_{ij} g_{ij}}{WN_0} \geq SNR_{\min}, \quad (9)$$

where SNR_{\min} refers to the required minimum Signal-to-Noise Ratio (SNR). On the other hand, when the node density is very high in nanonetworks, the interference from other communicating nodes should be considered, and it is expectedly much greater than the noise. Thus, the SINR can be given by:

$$\frac{P_{ij} g_{ij}}{\sum_{k \in \mathcal{N}, k \neq i} P_{kj} g_{kj}} \geq SIR_{\min}, \quad (10)$$

where SIR_{\min} refers to the required minimum Signal-to-Interference Ratio (SIR).

IV. AN UPPER BOUND ON NETWORK CAPACITY DUE TO NOISE

In this section, an information-theoretic approach is introduced to quantify the network capacity bounds of EM nanonetworks by taking into account the peculiarities of the THz-band channel, the required features of the THz physical and link layers, the nano-devices energy limitations and the need for multi-hop communication.

A. Single Link Capacity

Based on the system model introduced in Sec. III, and since the channel bandwidth of the THz band is arbitrarily large but finite, the Shannon capacity theorem is taken as a the starting point to analyze the network capacity. In the case of nanonetworks with a low node density, the capacity r_{ij} of each link with total noise WN_0 is upper bounded by

$$r_{ij} < W \log_2 \left(1 + \frac{P_{ij} g_{ij}}{WN_0} \right). \quad (11)$$

In order to establish the relations between the energy harvesting rate and network capacity, two metrics are proposed in this section: i) Energy efficiency, quantified by the energy per information bit $E_{ij} = \frac{P_{ij}}{r_{ij}}$ (in Joules per bit, J/bit), and ii) Spectrum efficiency, quantified by $C_{ij} = \frac{r_{ij}}{W}$ (in bits per second per Hertz, b/s/Hz). Based on the above two definitions, from (11), the energy efficiency and spectrum efficiency are related by the following condition

$$\frac{2^{C_{ij}} - 1}{C_{ij}} \frac{N_0}{g_{ij}} < E_{ij}. \quad (12)$$

The energy consumption rate of the link $X_i \rightarrow X_j$ is then given by $\lambda_{ij}^{cons} = E_{ij} r_{ij}$. From (7), the upper limit of the energy consumption rate over the link with the capacity r_{ij} can be computed as follows:

$$\lambda_{ij}^{cons} = \frac{2^{C_{ij}} - 1}{C_{ij}} N_0 r_{ij} |X_i - X_j|^{\alpha_{spr}} \exp(\alpha_{abs} |X_i - X_j|). \quad (13)$$

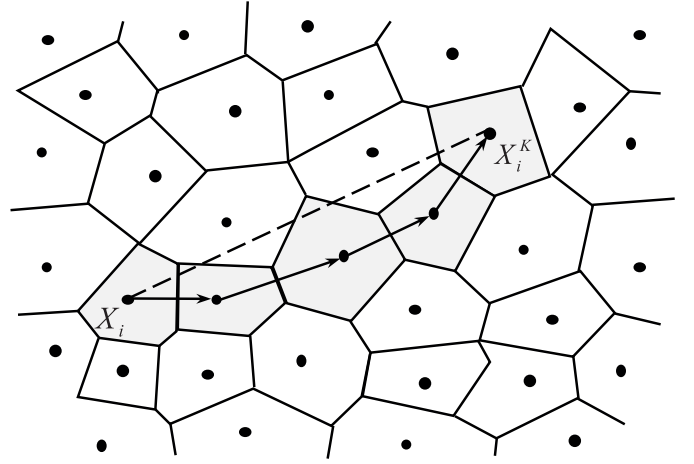


Fig. 2. Network topology and route R_i .

B. Multi-Hop Communication and Routing

The very limited transmission range of individual nano-devices forces the use of multi-hop links. In such scenario, the goal of a routing protocol is to identify the route to transfer data from the source node to the corresponding destination node that minimizes the energy consumption and maximizes the achievable throughput. We denote a route R_i from the source node X_i to the corresponding destination node X_i^K , as $R_i = [X_i^0, X_i^1, X_i^2, \dots, X_i^K]$ as shown in Fig. 2, where $X_i = X_i^0$ is the source node and K is the number of hops. Let $r_i(R_i)$ be the throughput achieved on the route R_i , which is given by

$$r_i(R_i) = \min \{r_i^{k,k-1} = WC_i^{k,k-1}\} \leq \frac{\sum_i r_i^{k,k-1}}{K}, \quad (14)$$

where $r_i^{k,k-1}$ ($k = 1, 2, \dots, K$) refers to the capacity of link from node X_i^k to node X_i^{k-1} on the route R_i . The throughput of route R_i equals to the minimum link capacity of all involved links, but is not greater than the average link capacity over total K links from the source to the destination. In detail, according to the channel model of THz signal, the path-loss of the typical link from node X_i^k to node X_i^{k-1} in the route R_i can be simplified as:

$$\left| X_i^k - X_i^{k-1} \right|^{\alpha_{spr}} \exp(\alpha_{abs} |X_i^k - X_i^{k-1}|). \quad (15)$$

Note that i) at each hop a packet is received, decoded, corrected, encoded and transmitted forward (i.e., it is not an amplify and forward but a decode and forward scheme) and ii) the main energy-consuming process at each hop is the actual transmission. Therefore, by combining (13) and (15), the total energy consumption rate over the route R_i can be obtained as

$$\lambda^{cons}(R_i) = N_0 \left(\sum_{k=1}^K r_i^{k,k-1} \frac{2^{C_i^{k,k-1}} - 1}{C_i^{k,k-1}} |X_i^k - X_i^{k-1}|^{\alpha_{spr}} \cdot \exp(\alpha_{abs} |X_i^k - X_i^{k-1}|) \right). \quad (16)$$

Without loss of generality, this total energy consumption rate is only an estimate of the equivalent energy that would be consumed over the route R_i .

C. Maximum Number of Nodes on the Route

We denote D_i as the Line-of-Sight (LoS) distance between the source X_i and the destination X_i^K , and L_i as the sum of the transmission distance over K hops, which can be given by

$$L_i \triangleq \sum_{k=1}^K |X_i^k - X_i^{k-1}| \geq D_i \triangleq |X_i^0 - X_i^K|. \quad (17)$$

Consider the network topology shown in Fig. 2, when there is a single-hop link or multiple hop links in the straight line between the source and the destination, the total transmission distance is $L_i = D_i$, otherwise, it is greater than D_i . However, due to the peculiarities of EM nanonetworks in the THz band, its transmission distance is extremely limited by the transmission power and the severe path loss, which also relies on the required performance of connectivity and coverage. Therefore, in order to explore the boundary of the achievable throughput of the route, the maximum number of nodes involved in the route requires to be investigated.

To elaborate, it is required to specify the routing scheme for the random THz nanonetworks based on some structure. Motivated by cellular architectures, a tessellation (covering by ‘‘cell’’) of the unit area is considered in this section as shown in Fig. 2, and which has been widely used for the analysis of network capacity [15], [16], [18]. According to the results of [16], every cell in the tessellation contains at most $50 \log n$ node with a big probability exceeding $\left(1 - \frac{50 \log n}{n}\right)$, where n refers to the number of nodes in the network. Thus, the maximum number of nodes on the route R_i is bounded as

$$N_{\max}^{\text{nodes}} \leq (C_1 \log n + C_2 L_i \sqrt{n \log n}), \quad (18)$$

where C_1 and C_2 are two different constants.

D. Harvested Energy With Two-State MAC Protocol

With the two-state MAC protocol described in Sec. III-C, the time interval in the HS state increases with different rules according to the value of the threshold W_{ts} , given by (5). The sum of time intervals in the HS state can be obtained as follows:

$$T_{\text{sum}} = \begin{cases} \sum_{i=1}^u 2T_i & T_u \leq W_{ts} \\ \sum_{i=1}^u 2T_i + \sum_{i=u+1}^v (T_i + 1) & T_u > W_{ts}, \end{cases} \quad (19)$$

where u is the maximum time for double increase period as time interval in the HS state is not greater than the threshold. Suppose the intermediate time of burst data appears in the v th cycle, then T_{sum} can be rewritten as follows:

$$T_{\text{sum}} = \begin{cases} 2^{u+1} - 1 & T_u \leq W_{ts} \\ 2^{u+1} - 1 + (v - u) \left(2^u + \frac{1+v-u}{2}\right) & T_u > W_{ts}. \end{cases} \quad (20)$$

Thus, the total energy harvested and stored by each nano-device in the consecutive HS state is $E_{\text{cap}}^{\text{HS}} = \lambda_{\text{harv}} T_{\text{sum}}$. Moreover, the maximum energy that can be stored is constrained by the storage capacity of nano-capacitor in nano-device, i.e., $E_{\text{cap}}^{\text{HS}} \leq E_{\text{max}}^{\text{harv}} = \frac{1}{2} C_{\text{cap}} V_g^2$ as shown in Sec. III-B. Hence, $E_{\text{cap}}^{\text{HS}}$ is bounded by:

$$E_{\text{cap}}^{\text{HS}} = \begin{cases} \lambda_{\text{harv}} T_{\text{sum}} & \lambda_{\text{harv}} T_{\text{sum}} \leq E_{\text{max}}^{\text{harv}} \\ E_{\text{max}}^{\text{harv}} & \lambda_{\text{harv}} T_{\text{sum}} > E_{\text{max}}^{\text{harv}}. \end{cases} \quad (21)$$

E. Upper Bound of Network Capacity

We denote $C_i^{k,k-1}$ as the spectrum efficiency of link between node X_i^k and node X_i^{k-1} on the route R_i , $r(n)$ as the upper bound of the achievable throughput, C as the corresponding spectrum efficiency with the upper bound throughput, i.e., $C = \frac{r(n)}{W}$. According to (16), the total energy consumption rate on route R_i is bounded by (22), as shown at the bottom of this page, where (22-a) is because of the following reasons: i) the convexity of $|X_i^k - X_i^{k-1}|^{\alpha_{\text{spr}}}$ for $\alpha_{\text{spr}} \geq 1$, ii) the monotonically increasing natural exponential function $\exp(x)$, iii) $C \leq C_i^{k,k-1}$ as a result of $r(n) \leq r_i^{k,k-1}$, $1 \leq K \leq N_{\max}^{\text{nodes}}$ and iv) the observation from (17). (22-b) is from Equation (18). (22-c) is from defining a new function of total transmission distance L_i and the number of nodes n , i.e., $f(L_i, n) \triangleq \frac{L_i^{\alpha_{\text{spr}}}}{(C_1 \log n + C_2 L_i \sqrt{n \log n})^{\alpha_{\text{spr}}}} \exp\left(\frac{\alpha_{\text{abs}} L_i}{C_1 \log n + C_2 L_i \sqrt{n \log n}}\right)$.

According to the limited energy harvesting rate and maximum energy storage capacity in Sec. III-B, the energy is constrained by each nano-device, not the whole route R_i or nanonetwork. Therefore, as a final step, the average consumed energy by each nano-device involved in the route R_i is bounded by the maximum transmission power P_0 multiplied by the total transmission time, and also bounded by the harvested energy during the time period in HS state and HTR state, i.e., $\lambda_{\text{harv}} (T_{\text{sum}} + T_{\text{tr}})$, where T_{tr} is the required time of transmission, which depends on the number of data packets needed to be delivered.

Finally, the relation between the energy harvesting and consumption can be presented in (23), as shown at the bottom of the next page, where $\mathbb{E}()$ refers to the average function. (23-a) is from (22-c), $K \leq N_{\max}^{\text{nodes}}$ and the fact that $f(L_i, n)$ is an increasing function of L_i as n is fixed and $L_i \geq D_i$, $\hat{f}(D_i, n) \triangleq \frac{D_i^{\alpha_{\text{spr}}}}{(C_1 \log n + C_2 D_i \sqrt{n \log n})^{\alpha_{\text{spr}}-1}} \cdot \exp\left(\frac{\alpha_{\text{abs}} D_i}{C_1 \log n + C_2 D_i \sqrt{n \log n}}\right)$. According to the definition of function $\hat{f}(D_i, n)$, due to the relation of $C_1 \log n \leq C_1 \sqrt{n \log n}$, then the term $(C_1 \log n + C_2 D_i \sqrt{n \log n})^{\alpha_{\text{spr}}-1} \leq (C_3 \sqrt{n \log n})^{\alpha_{\text{spr}}-1}$, i.e., $C_3 = C_1 + C_2 D_i$, which results in (23-b).

Since $\mathbb{E}(D_i)$ becomes a constant as n becomes large, the mean distance between two randomly selected nodes (source-destination pair) in a disk of unit area is approximate to 0.5

$$\lambda^{\text{cons}}(R_i) = N_0 \left(\sum_{k=1}^K \frac{2^{C_i^{k,k-1}} - 1}{C_i^{k,k-1}} r_i^{k,k-1} |X_i^k - X_i^{k-1}|^{\alpha_{\text{spr}}} \exp\left(\alpha_{\text{abs}} |X_i^k - X_i^{k-1}|\right) \right) \quad (22)$$

in [17]. Thus, (23) can be rewritten as follows:

$$\frac{2^C - 1}{C} r(n) \leq \lambda_{harv} \left(\frac{T_{sum} + T_{tr}}{T_{tr}} \right) \frac{C_4 (n \log n)^{\frac{a_{spr}-1}{2}}}{\exp\left(\frac{C_5 \alpha_{abs}}{\sqrt{n \log n}}\right)}, \quad (24)$$

while with constraint $\lambda_{harv} T_{sum} \leq E_{max}^{harv}$. According to the definition of spectrum efficiency given by (12) and Taylor series of 2^C , the upper bound on network capacity is given by (25), as shown at the bottom of the next page, by substituting $C = \frac{r}{W}$ and $\left(2^C - 1 = \ln 2 \cdot C + \frac{(\ln 2)^2}{2} C^2\right)$, where (25-a) is from the inequality of $\sqrt{a+b} \leq \sqrt{a} + \sqrt{b}$. Moreover, the consumed energy over transmission time is upper bounded by the maximum transmission power P_0 and lower bounded by the harvesting rate, i.e., $\lambda_{harv} \leq P_{tr} \leq P_0$. It is observed that both the spreading loss and molecular absorption loss have a significant effect on the network capacity, as well as the energy harvesting process and pulse-based modulation. This result provides a guideline for the design of the future THz nanonetworks.

Without loss of generality, as $n \rightarrow \infty$ and the transmission power P_{tr} is bounded by P_0 , the upper bound of network capacity can be presented as follows:

$$\begin{aligned} r(n) &= O\left(W P_0 \frac{(n \log n)^{\frac{a_{spr}-1}{2}}}{\exp\left(\frac{\alpha_{abs}}{\sqrt{n \log n}}\right)}\right)^{\frac{1}{2}} \\ &= O\left(W P_0 (n \log n)^{\frac{a_{spr}-1}{2}}\right)^{\frac{1}{2}}, \end{aligned} \quad (26)$$

where (26) is from the conclusion given by (25) without considering the effect of constants, (26-a) is from the special case of without considering the molecular absorption loss in THz communication.

V. AN UPPER BOUND OF NETWORK CAPACITY DUE TO INTERFERENCE

In Sec. IV, an upper bound on network capacity of THz nanonetworks without considering the interference is presented. However, in light of the very high node density in

the envisioned applications and by considering the simultaneous transmission among the huge number of nano-devices, collisions between the transmitted symbols may occur. In [10], multi-user interference in nanonetworks when utilizing a THz pulse-based Time-Spread On-Off Keying (TS-OOK) modulation was investigated. In particular, it was shown that the transmission using very short pulses, just hundreds of femtoseconds long, enables simultaneous transmissions between uncoordinated nodes at up to several gigabits-per-second (Gbps) each. However, it was also shown that, as the number of nanonodes increases, interference plays the major role. Therefore, the interference as a result of collisions should be considered under these conditions, which leads to a limitation on the capacity of nanonetworks.

To investigate the impact of interference on the network capacity performance, suppose the interference plays a dominant role in the SINR, and the introduced noise is negligible, i.e., $\sum_{k \in \mathcal{N}, k \neq i} P_{kj} g_{kj} \geq N_0 W$. Thus, (11) can be rewritten as follows:

$$r_{ij} < W \log_2 \left(1 + \frac{P_{ij} g_{ij}}{\sum_{k \in \mathcal{N}, k \neq i} P_{kj} g_{kj}} \right). \quad (27)$$

Without loss of generality, for transmission distances up to one meter, for a signal transmitted from the node k , its reception power at the receiver can be approximated by the polynomial [29]:

$$P_{kj} g_{kj} \approx \beta_1 (d_{kj})^{-\beta_2}, \quad (28)$$

where β_1 and β_2 are two constants which depend on the specific channel molecular composition and the transmitted signal. Under a standard medium composition, pulse energy $E_p = 0.1$ aJ in the TS-OOK modulation [10], the values of these two constants are $\beta_1 \approx 1.39 \times 10^{-18}$ and $\beta_2 \approx 2.1$. From [29], the p.d.f. of the interference power is given by

$$f_I(i) = \frac{1}{\pi i} \sum_{k=1}^{\infty} \frac{\Gamma(\gamma k + 1)}{k!} \left(\frac{\pi \lambda' \beta_1 \Gamma(1 - \gamma)}{i^\gamma} \right)^k \cdot \text{sinc} \pi(1 - \gamma), \quad (29)$$

where $\Gamma()$ stands for the gamma function, $\gamma = 2/\beta_2 \approx 0.95$. λ' refers to the Poisson process parameter in nodes/m², which

$$\geq \frac{2^C - 1}{C} N_0 r(n) \left(\frac{L_i}{N_{max}^{nodes}} \right)^{a_{spr}} \exp\left(\alpha_{abs} \frac{L_i}{N_{max}^{nodes}}\right) \quad (22-a)$$

$$\geq \frac{2^C - 1}{C} N_0 r(n) \frac{L_i^{a_{spr}}}{(C_1 \log n + C_2 L_i \sqrt{n \log n})^{a_{spr}}} \exp\left(\frac{\alpha_{abs} L_i}{C_1 \log n + C_2 L_i \sqrt{n \log n}}\right) \quad (22-b)$$

$$\geq \frac{2^C - 1}{C} N_0 r(n) f(L_i, n) \quad (22-c)$$

$$E_{max}^{harv} + \lambda_{harv} T_{tr} \geq E_{cap}^{HS} + \lambda_{harv} T_{tr} = \lambda_{harv} (T_{sum} + T_{tr}) \geq \mathbb{E}\left(\frac{\lambda^{cons}(R_i)}{K}\right) \cdot T_{tr} \quad (23)$$

$$\geq \frac{2^C - 1}{C} N_0 r(n) \mathbb{E}\left(\frac{f(D_i, n)}{N_{max}^{nodes}}\right) \cdot T_{tr} = \frac{2^C - 1}{C} N_0 r(n) \mathbb{E}\left(\hat{f}(D_i, n)\right) \cdot T_{tr} \quad (23-a)$$

$$\geq \frac{2^C - 1}{C} N_0 r(n) \left(\frac{\mathbb{E}(D_i)^{a_{spr}}}{(C_3 \sqrt{n \log n})^{a_{spr}-1}} \exp\left(\frac{\alpha_{abs} \mathbb{E}(D_i)}{C_3 \sqrt{n \log n}}\right) \right) \cdot T_{tr} \quad (23-b)$$

can be calculated as $\lambda' = n (2T_p/T_s) p_1$ (where n refers to the number of nodes), T_p refers to the symbol length, T_s refers to the time between two consecutive symbols, and p_1 refers to the probability of transmitting one pulse. According to the TS-OOK modulation, with the values of T_p/T_s and p_1 , the average interference power $I(n)$ can be calculated as follows:

$$I(n) = \frac{1}{\pi} \sum_{i=0}^{\infty} \sum_{k=1}^{\infty} \frac{\Gamma(\gamma k + 1)}{k!} \left(\frac{\pi \beta_1 \Gamma(1 - \gamma) 2T_p p_1 n}{i^\gamma T_s} \right)^k \times \text{sinc} \pi(1 - \gamma). \quad (30)$$

By combining (27) and (30), the total energy consumption rate over the route R_i by considering the interference is rewritten as

$$\lambda_I^{\text{cons}}(R_i) = I(n) \left(\sum_{k=1}^{k=K} \left(2^{C_i^{k,k-1}} - 1 \right) \left| X_i^k - X_i^{k-1} \right|^{\alpha_{spr}} \cdot \exp \left(\alpha_{abs} \left| X_i^k - X_i^{k-1} \right| \right) \right). \quad (31)$$

Similar to the derivations of the network capacity in Sec. IV-E, the upper bound of network capacity with the interference is given by (32), as shown at the bottom of this page.

Without loss of generality, as $n \rightarrow \infty$ and the transmission power P_{tr} is bounded by P_0 , the upper bound with the interference can be presented as follows:

$$r_I(n) = O \left(\frac{W^2 P_0 (n \log n)^{\frac{\alpha_{spr}-1}{2}}}{I(n) \exp \left(\frac{\alpha_{abs}}{\sqrt{n \log n}} \right)} \right)^{\frac{1}{2}} \quad (33)$$

$$= O \left(\frac{W^2 P_0}{I(n)} (n \log n)^{\frac{\alpha_{spr}-1}{2}} \right)^{\frac{1}{2}}, \quad (33\text{-a})$$

where (33) results from (32) without considering the effect of constants, (33-a) is from the special case of without considering the molecular absorption loss in THz communication. It is observed that when the node density is very high,

TABLE I
SYMBOL VALUES

| Symbols | Values |
|---------|---|
| C_1 | 4800 |
| C_2 | 136 |
| C_3 | $C_1 + C_2 D_i$ |
| C_4 | $(C_3)^{\alpha_{spr}-1} / N_0 \mathbb{E}(D_i)^{\alpha_{spr}}$ |
| C_5 | $\mathbb{E}(D_i) / C_3$ |

besides the peculiarities of THz band and energy limitation, the interference between nano-devices plays a key role.

VI. PERFORMANCE ASSESSMENT

In this section, a detailed analysis on the network capacity in THz nanonetworks is presented. In detail, our developed bounds as well as the results in the existing literature, such as Gupta's capacity in [15], Negi's capacity in [16] and Tang's capacity in [17], are shown in Fig. 3. Gupta's work was taken into account the impact of the spreading loss in the propagation of traditional wireless signals, and considered the nodes have endless energy and unbound transmission power. As a result of the non-interference protocol, Gupta's capacity decreases with node density. Based on Gupta's result and Shannon capacity formula, Negi and Rajeswaran [17] and Tang and Hua [18] investigated the capacity of energy-constrained wireless networks with the assumption of unlimited bandwidth, which results in the lack of multi-user interference. Under these conditions, the capacities in their results increase with node density n , compared with Gupta's result. Moreover, the difference between Negi's result and Tang's result is caused by using different mathematic skills, but they both take an approximation of the Shannon capacity formula as a linear function. For the illustration, we have used the values of the channel model in [8], the TS-OOK modulation [10] and the energy harvesting system in [12]. In detail, the used in the simulations are presented in Table I.

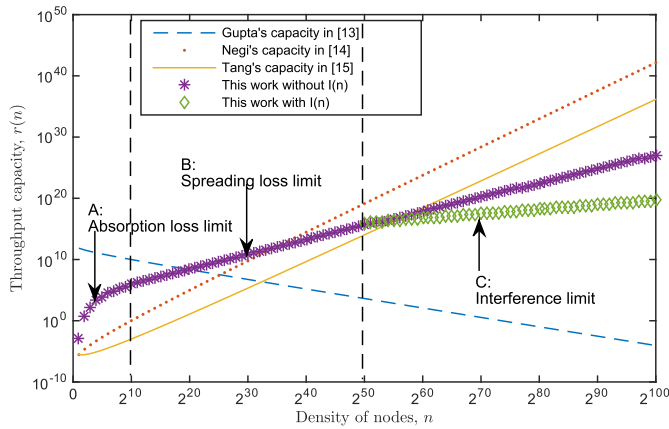
In this paper, in terms of path loss, the spreading loss and molecular absorption loss are both considered for THz

$$r(n) \leq \frac{W}{\ln 2} \left(\sqrt{1 + \frac{2}{W} \left(\lambda_{harv} \left(\frac{T_{sum} + T_{tr}}{T_{tr}} \right) \frac{C_4 (n \log n)^{\frac{\alpha_{spr}-1}{2}}}{\exp \left(\frac{C_5 \alpha_{abs}}{\sqrt{n \log n}} \right)} \right) - 1} \right) \quad (25)$$

$$\leq \frac{\sqrt{2W}}{\ln 2} \left(P_{tr} \frac{C_4 (n \log n)^{\frac{\alpha_{spr}-1}{2}}}{\exp \left(\frac{C_5 \alpha_{abs}}{\sqrt{n \log n}} \right)} \right)^{\frac{1}{2}} \quad (25\text{-a})$$

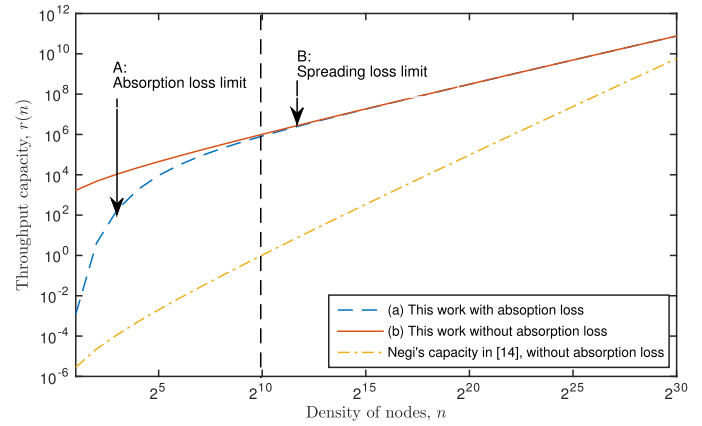
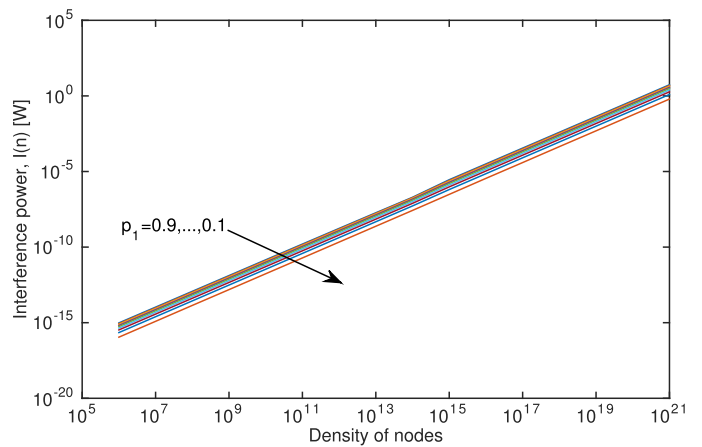
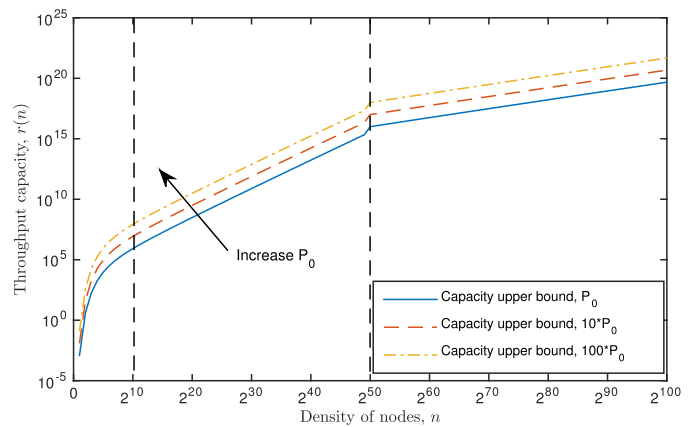
$$r_I(n) \leq \frac{W}{\ln 2} \left(\sqrt{1 + \frac{2}{I(n)} \left(\lambda_{harv} \left(\frac{T_{sum} + T_{tr}}{T_{tr}} \right) \frac{C_4 (n \log n)^{\frac{\alpha_{spr}-1}{2}}}{\exp \left(\frac{C_5 \alpha_{abs}}{\sqrt{n \log n}} \right)} \right) - 1} \right) \quad (32)$$

$$\leq \frac{\sqrt{2W}}{\ln 2} \left(\frac{P_{tr}}{I(n)} \frac{C_4 (n \log n)^{\frac{\alpha_{spr}-1}{2}}}{\exp \left(\frac{C_5 \alpha_{abs}}{\sqrt{n \log n}} \right)} \right)^{\frac{1}{2}} \quad (32\text{-a})$$

Fig. 3. Throughput capacity $r(n)$.

nanonetworks. From the aspect of energy constraints, maximum transmission power, limited energy harvesting rate and limited energy store capacity are all considered in each node of nanonetworks. Moreover, two metrics, energy efficiency and spectrum efficiency, are introduced to solve the Shannon capacity formula, and achieve a strictly tighter upper bound than other three models. Therefore, it is observed that the upper bound of network capacity can be divided into three phases with the increase of node density as shown in Fig. 3. Phase A indicates that molecular absorption loss dominates the influence on the network capacity in case of low node density, i.e., the achievable throughput is mainly limited by the absorption loss in Phase A. When the node density is raised, the spreading loss has a main influence on the network capacity as a result of significant multi-hops, which means that in Phase B, the spreading loss significantly limits the achievable throughput. When the node density is extremely high, the interference among nodes should be considered. While the THz band provides nodes with a huge bandwidth and TS-OOK enables the interleaving of a very large number of users, the bandwidth is limited and multi-user interference dominates this Phase C. Please note that the transition between phases in the figures, depends on the actual values of the channel propagation model, communication parameters (Physical layer, MAC layer), and the energy harvesting capabilities (harvesting rate, energy capacity).

According to the developed bounds given by (26), especially for nanonetworks with low densities, a detailed analysis of throughput bounds is given in Fig. 4. In a unified area, molecular absorption loss has a significant impact on the achievable throughput when network density is smaller than 2^{10} , which results in the exponential increase in Phase A. With the increase of network density, more number of nodes are involved in each route, one hop transmission distance is reduced, then spreading loss dominates the achievable throughput, and also contributes to its approximately linear improvement. Moreover, the molecular absorption loss coefficient as a function of frequency has some peak points at some specific frequency points. Especially under the condition of long transmission distance, these peak points should be avoided to alleviate the molecular absorption loss.

Fig. 4. Throughput capacity $r(n)$.Fig. 5. Interference power $I(n)$.Fig. 6. Throughput capacity with interference $r_l(n)$.

With the increase of node density in nanonetworks, the interference power among nano-devices is demonstrated in Fig. 5, which verifies the conclusion given by (33) of Sec. V, i.e., the interference should be taken into consideration of the capacity in nanonetworks with high node density. It is observed that the interference power exponentially increases with node density, which will limit the node density in the applications of nanonetworks. However, systems and

mechanisms with adaptive power control can be utilized to alleviate the impact of interference.

Fig. 6 presents the whole upper bound of network capacity from three phases under different node densities and transmission powers. Intuitively, the network capacity increases with the addition of maximum transmission power. This addition will not change the shape of the bound, just shift the throughput curves. Moreover, the same to the effect of noise on the proposed model given by (25-a) and (32-a). It is because we keep the proposed model and analysis general to remain valid even as technology advances or parameter value changes. Obviously, the presented bound has a better and more reasonable performance both in cases of high or low node density. Therefore, we present a strictly tighter upper bound on the achievable throughput of THz nanonetworks, which can be used as a guideline to design the future nanonetworks.

VII. CONCLUSION

According to the limited size of nanodevices, scaling a metallic antenna down to a few hundred nanometers would impose the use of very high operating frequencies. THz band can be realized to radiate with the benefits of graphene and its derivatives. However, the traditional RF communication mechanisms on the basis of continuous transmission signals would be not suitable for nanonetworks with limited hardware. Network capacity is one of the main parameters for the design and evaluation of wireless networks. In this paper, the network capacity of power-constrained nanonetworks is comprehensively analyzed by considering the peculiarities of THz Band and energy limitation of nano-devices. With the proposed two-state MAC protocol, for a nanonetwork consisting of n randomly distributed identical nodes over a unit area, the upper bounds of achievable throughput $r(n)$ with different node densities are presented.

From the above results, it is observed that the whole upper boundary can be separated into three phases. In nanonetworks with low density, the molecular absorption loss dramatically alters the achievable throughput; while in nanonetworks with high density, the absorption loss is not the main factor, the interference among nodes dominates the achievable throughput. In detail, the throughput decreases with the molecular absorption loss coefficient, which indicates some frequency sub-bands with high absorption loss should be avoided. This analysis will guide the design of future nanonetworks to achieve a better performance.

REFERENCES

- [1] I. F. Akyildiz and J. M. Jornet, "Electromagnetic wireless nanosensor networks," *Nano Commun. Netw.*, vol. 1, no. 1, pp. 3–19, Mar. 2010.
- [2] A. Afsharinejad, A. Davy, B. Jennings, and C. Brennan, "Performance analysis of plant monitoring nanosensor networks at THz frequencies," *IEEE Internet Things J.*, vol. 3, no. 1, pp. 59–69, Feb. 2016.
- [3] F. H. L. Koppens, D. E. Chang, and F. J. Garcia de Abajo, "Graphene plasmonics: A platform for strong light–matter interactions," *Nano Lett.*, vol. 11, no. 8, pp. 3370–3377, Aug. 2011.
- [4] J. M. Jornet and I. F. Akyildiz, "Graphene-based plasmonic nano-antenna for terahertz band communication in nanonetworks," *IEEE J. Sel. Areas Commun.*, vol. 31, no. 12, pp. 685–694, Dec. 2013.
- [5] A. P. Shrestha, S. J. Yoo, H. J. Choi, and K. S. Kwak, "Enhanced rate division multiple access for electromagnetic nanonetworks," *IEEE Sensors J.*, vol. 16, no. 19, pp. 7287–7296, Oct. 2016.
- [6] I. F. Akyildiz, J. M. Jornet, and C. Han, "Terahertz band: Next frontier for wireless communications," *Phys. Commun.*, vol. 12, pp. 16–32, Sep. 2014.
- [7] X.-W. Yao and J. M. Jornet, "TAB-MAC: Assisted beamforming MAC protocol for terahertz communication networks," *Nano Commun. Netw.*, vol. 9, pp. 36–42, Sep. 2016.
- [8] J. M. Jornet and I. F. Akyildiz, "Channel modeling and capacity analysis for electromagnetic wireless nanonetworks in the terahertz band," *IEEE Trans. Wireless Commun.*, vol. 10, no. 10, pp. 3211–3221, Oct. 2011.
- [9] C. Han, A. O. Bicen, and I. F. Akyildiz, "Multi-ray channel modeling and wideband characterization for wireless communications in the terahertz band," *IEEE Trans. Wireless Commun.*, vol. 14, no. 5, pp. 2402–2412, May 2015.
- [10] J. M. Jornet and I. F. Akyildiz, "Femtosecond-long pulse-based modulation for terahertz band communication in nanonetworks," *IEEE Trans. Commun.*, vol. 62, no. 5, pp. 1742–1754, May 2014.
- [11] Z. L. Wang, "Towards self-powered nanosystems: From nanogenerators to nanopiezotronics," *Adv. Funct. Mater.*, vol. 18, no. 22, pp. 3553–3567, 2008.
- [12] J. M. Jornet and I. F. Akyildiz, "Joint energy harvesting and communication analysis for perpetual wireless nanosensor networks in the terahertz band," *IEEE Trans. Nanotechnol.*, vol. 11, no. 3, pp. 570–580, May 2012.
- [13] X.-W. Yao, W.-L. Wang, and S.-H. Yang, "Joint parameter optimization for perpetual nanonetworks and maximum network capacity," *IEEE Trans. Mol. Biol. Multi-Scale Commun.*, vol. 1, no. 4, pp. 321–330, Dec. 2015.
- [14] S. Weber, J. G. Andrews, and N. Jindal, "An overview of the transmission capacity of wireless networks," *IEEE Trans. Commun.*, vol. 58, no. 12, pp. 3593–3604, Dec. 2010.
- [15] P. Gupta and P. R. Kumar, "The capacity of wireless networks," *IEEE Trans. Inf. Theory*, vol. 46, no. 2, pp. 388–404, Mar. 2000.
- [16] R. Negi and A. Rajeswaran, "Capacity of power constrained ad-hoc networks," in *Proc. 23rd Annu. Joint Conf. IEEE Comput. Commun. Soc. (INFOCOM)*, vol. 1, Mar. 2004, p. 453.
- [17] X. Tang and Y. Hua, "Capacity of ultra-wideband power-constrained ad hoc networks," *IEEE Trans. Inf. Theory*, vol. 54, no. 2, pp. 916–920, Feb. 2008.
- [18] S. Yi, Y. Pei, and S. Kalyanaraman, "On the capacity improvement of ad hoc wireless networks using directional antennas," in *Proc. 4th ACM Int. Symp. Mobile Ad Hoc Netw. (MobiHoc)*, New York, NY, USA, 2003, pp. 108–116.
- [19] P. Li, C. Zhang, and Y. Fang, "The capacity of wireless ad hoc networks using directional antennas," *IEEE Trans. Mobile Comput.*, vol. 10, no. 10, pp. 1374–1387, Oct. 2011.
- [20] D. Xie, W. Wei, Y. Wang, and H. Zhu, "Tradeoff between throughput and energy consumption in multirate wireless sensor networks," *IEEE Sensors J.*, vol. 13, no. 10, pp. 3667–3676, Oct. 2013.
- [21] S. Singh, R. Mudumbai, and U. Madhow, "Interference analysis for highly directional 60-GHz mesh networks: The case for rethinking medium access control," *IEEE/ACM Trans. Netw.*, vol. 19, no. 5, pp. 1513–1527, Oct. 2011.
- [22] P. Boronin, V. Petrov, D. Moltchanov, Y. Koucheryavy, and J. M. Jornet, "Capacity and throughput analysis of nanoscale machine communication through transparency windows in the terahertz band," *Nano Commun. Netw.*, vol. 5, no. 3, pp. 72–82, 2014.
- [23] X. Wang, J. Song, J. Liu, and Z. L. Wang, "Direct-current nanogenerator driven by ultrasonic waves," *Science*, vol. 316, pp. 102–105, Apr. 2007.
- [24] C. Xu, C. Pan, Y. Liu, and Z. L. Wang, "Hybrid cells for simultaneously harvesting multi-type energies for self-powered micro/nanosystems," *Nano Energy*, vol. 1, no. 2, pp. 259–272, 2012.
- [25] J. M. Jornet, J. C. Pujol, and J. S. Pareta, "PHLAME: A physical layer aware MAC protocol for electromagnetic nanonetworks in the terahertz band," *Nano Commun. Netw.*, vol. 3, no. 1, pp. 74–81, 2012.
- [26] S. Mohrehkesh, M. C. Weigle, and S. K. Das, "DRIH-MAC: A distributed receiver-initiated harvesting-aware MAC for nanonetworks," *IEEE Trans. Mol. Biol. Multi-Scale Commun.*, vol. 1, no. 1, pp. 97–110, Mar. 2015.
- [27] N.-H. Lee and S. Bahk, "MAC sleep mode control considering downlink traffic pattern and mobility," in *Proc. Proc. IEEE 61st Veh. Technol. Conf. (VTC-Spring)*, vol. 3, May 2005, pp. 2076–2080.

- [28] A. P. Azad, S. Alouf, E. Altman, V. Borkar, and G. S. Paschos, "Optimal control of sleep periods for wireless terminals," *IEEE J. Sel. Areas Commun.*, vol. 29, no. 8, pp. 1605–1617, Sep. 2011.
- [29] J. M. Jornet and I. F. Akyildiz, "Low-weight channel coding for interference mitigation in electromagnetic nanonetworks in the terahertz band," in *Proc. IEEE Int. Conf. Commun. (ICC)*, Jun. 2011, pp. 1–6.

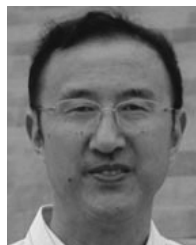


Xin-Wei Yao (M'14) received the B.S. degree in mechanical and electrical engineering and the Ph.D. degree in information engineering from Zhejiang University of Technology (ZJUT), Hangzhou, China, in 2008 and 2013, respectively. From 2012 to 2013, he was a Visiting Scholar with Loughborough University, Leicestershire, U.K. From 2015 to 2016, he was a Visiting Professor with the University of Buffalo, The State University of New York, Buffalo, NY, USA. He is currently an Associate Professor with the College of Computer Science and Technology, ZJUT.

His current research interests are in the area of terahertz-band communication networks, electromagnetic nanonetworks, wireless ad hoc and sensor networks, wireless power transfer, and the Internet of Things. He is a member of the ACM. He has served on technical program committees of many IEEE/ACM conferences. He was a recipient of the Outstanding Doctoral Thesis Award and the Distinguished Associate Professor Award from ZJUT in 2013 and 2014, respectively.



Chao-Chao Wang received the bachelor's degree in computer science and technology from the Zhejiang University of Technology, Hangzhou, China, in 2014, where he is currently pursuing the Ph.D. degree in control science and engineering. His current research interests include terahertz band communication networks, electromagnetic nanonetwork, wireless ad hoc sensor networks, Internet of Things, and 5G cellular networks.



Wan-Liang Wang received the Ph.D. degree in control theory and control engineering from Tongji University, Shanghai, China, in 2001. In 2002, he visited The University of Manchester Institute of Science and Technology and Loughborough University, U.K. In 2007, he visited the Georgia Institute of Technology and the University of Michigan, USA. He is currently a Full Professor with the Zhejiang University of Technology, Hangzhou, China. His research interests include computer networks, networked control, Internet of Things and artificial intelligence. He was a recipient of the National Outstanding Teacher Award and the First National Teacher of Ten Thousand Plan Award, in 2008 and 2014, respectively.



Josep Miquel Jornet received the B.S. degree in telecommunication engineering and the M.Sc. degree in information and communication technologies from the Universitat Politècnica de Catalunya, Barcelona, Spain, in 2008, and the Ph.D. degree in electrical and computer engineering from the Georgia Institute of Technology, Atlanta, GA, USA, in 2013. From 2007 to 2008, he was a Visiting Researcher with the Massachusetts Institute of Technology (MIT), Cambridge, under the MIT Sea Grant program. He is currently an Assistant Professor with the Department of Electrical Engineering, University at Buffalo (UB), The State University of New York.

His current research interests are in terahertz-band communication networks, nanophotonic wireless communication, intra-body wireless nanosensor networks and the Internet of Nano-Things. He is a member of the ACM. In 2016 and 2017, he received the Distinguished TPC Member Award at the IEEE International Conference on Computer Communications. In 2017, he received the IEEE Communications Society Young Professional Best Innovation Award, the ACM NanoCom Outstanding Milestone Award, and the UB SEAS Early Career Researcher of the Year Award. Since 2016, he has been the Editor-in-Chief of the *Nano Communication Networks* (Elsevier) Journal, and also serves in the Steering Committee of the ACM Nanoscale Computing and Communications Conference Series.